JACS
JOURNAL OF THE AMERICAN CHEMICAL SOCIETY
Communication
pubs.acs.org/JACS

Analyzing Amyloid Beta Aggregates with a Combinatorial Fluorescent Molecular Sensor

Joydev Hatai, Leila Motiei, and David Margulies*

Department of Organic Chemistry, Weizmann Institute of Science, Rehovot 7610001, Israel

Supporting Information

ABSTRACT: Different amyloid beta (Aβ) aggregates can be discriminated by a combinatorial fluorescent molecular sensor. The unique optical fingerprints generated by the unimolecular analytical device provide a simple means to differentiate among aggregates generated from different alloforms or through distinct pathways. The sensor has also been used to track dynamic changes that occur in Aβ aggregation states, which result from the formation of low molecular weight oligomers, high molecular weight oligomers, protofibrils, and fibrils.

The aggregation of amyloid beta (Aβ) peptides (Figure 1a) is thought to play a major role in the progression of

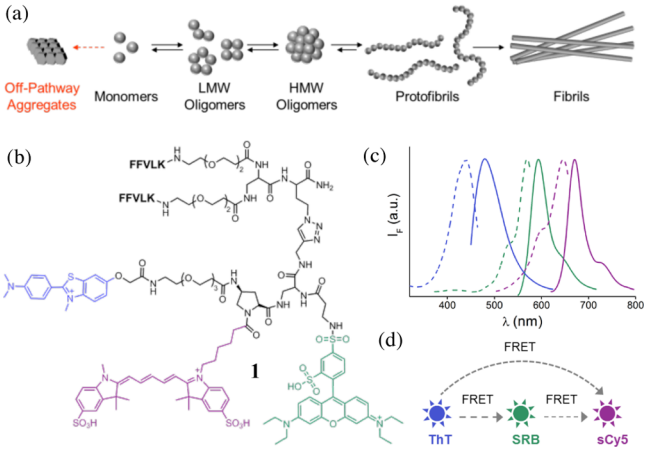

Figure 1. (a) Schematic representation of the Aβ aggregation process. (b) Chemical structure of a combinatorial fluorescent molecular sensor **1** that integrates two Aβ aggregate binders: ThT and bis-KLVFF peptide, and three fluorescent reporters: ThT (blue), SRB (green), and sCy5 (magenta). (c) Normalized excitation (dotted line) and emission spectra (solid line) of ThT (with Aβ fibrils), SRB, and sCy5. (d) FRET processes that can occur when exciting **1** at 440 nm.

Alzheimer's disease. Much effort has therefore been made in investigating the composition of Aβ assemblies, the mechanism underlying fibril formation, and the parameters that could affect Aβ toxicity.[1] It has been shown, for example, that Aβ aggregates can be generated via different pathways[1a,b] and that low molecular weight (LMW) oligomers greatly contribute to neurotoxicity.[1c] It has also been demonstrated that Aβ aggregates can be assembled from different alloforms, such as Aβ_{40} and Aβ_{42}, which differ in their length and concentrations and may have different toxicities.[1d,e]

Although these studies indicate that subtle variations in the dynamics and compositions of Aβ aggregates could have a significant impact on their physicochemical and pathological properties, currently there is no effective means to characterize straightforwardly the Aβ aggregation state. The widely used fluorescence assay based on Thioflavin T (ThT),[2] for example, which can readily sense fibril formation, cannot distinguish among alloforms and is unsuitable for identifying different intermediates in the mixture. Similarly, recently developed fluorescent probes with notable selectivity toward oligomers[3] or fibril types[4] provide only partial information about the composition of Aβ assemblies. Combining distinct probes has been cleverly used to detect cysteine-modified oligomers and fibrils simultaneously,[5] indicating the potential for tracking additional, unmodified Aβ aggregates, with relatively simple fluorescent assays. Other techniques[6] such as mass spectrometry, gel electrophoresis, immunoblotting, or using rationally designed peptides[7] can effectively determine the composition of Aβ aggregates. These methods, however, require special expertise and are not high-throughput.

An alternative methodology that has been used to analyze mixtures of peptides or proteins is differential sensing[8] (or the "nose/tongue" approach). Unlike most small molecule-based sensors, which are designed to detect specific analytes, differential sensors generally consist of arrays of probes that are cross-reactive. The lack of specificity enables such systems to interact with various components in the mixtures and generate a wide range of identification patterns, akin to the way the olfactory system operates.[8a] We have recently developed unimolecular, pattern-generating sensors, termed combinatorial fluorescent molecular sensors,[9] which combine several synthetic receptors and fluorescent reporters. It occurred to us that providing such a sensor with the ability to interact with different Aβ aggregate species (e.g., LMW oligomers, high molecular weight (HMW) oligomers, protofibrils, and fibrils) should enable it to track dynamic changes that occur in Aβ aggregation states, as well as to discriminate among aggregates generated from distinct alloforms or through different pathways.

The structure of a combinatorial sensor for Aβ aggregates (Figure 1b, **1**) consists of a *cis*-amino proline scaffold that is appended with three fluorescent reporters: thioflavin T (ThT), sulforhodamine B (SRB), and sulfo-Cy5 (sCy5) that serve as a FRET donor 1-(acceptor 1/donor 2)-acceptor 2 system. Such

Received: October 16, 2016
Published: February 7, 2017

DOI: 10.1021/jacs.6b10809
J. Am. Chem. Soc. 2017, 139, 2136−2139

intramolecular FRET processes have been shown to enhance the efficiency of pattern-generating devices.[9,10] On the basis of the excitation and emission spectra of the individual dyes (Figure 1c), we expected that illuminating **1** at 440 nm would excite the ThT dye and that the resulting fluorescence would also trigger the emission of SRB and sCy5, owing intramolecular communication among ThT-SRB, ThT-sCy5, and SRB-sCy5 FRET pairs (Figure 1d). In addition, the sensor contains two amyloid binders: a bis-KLVFF peptide[7] and ThT. The first should enable it to bind LMW oligomers,[7] whereas the second can interact with fibrils[2] and has also been shown to bind protofibrils and HMW oligomers.[2,11]

Notably, even without these binders, such a large and flexible molecule with various polar, hydrophobic, and charged groups (Figure 1b) should be able to interact nonspecifically with various Aβ aggregate types. We expected, however, that the specific binders (i.e., ThT and bis-KLVFF peptide) would improve the discriminating ability of **1** by increasing its binding affinities and diversifying its fluorescence responses. The emission of ThT[2] and its derivatives, for example, is enhanced upon binding to fibrils, and they may also respond to HMW oligomers[11a] and to protofibrils.[11b] Owing to FRET communication between ThT and SRB, as well as between ThT and sCy5 (Figure 1c), these interactions should also enhance the emission of SRB and sCy5 even if their emission is not directly affected by these aggregates (Figure 1c). In another scenario, the binding of **1** to different aggregate species, including LMW oligomers, would distance ThT from SRB and sCy5, which would reduce FRET efficiency and decrease the acceptors' emission intensity. Quenching by amino acid side chains or neighboring dyes are additional factors that could alter the emission patterns.

Initially, we tested the ability of **1** to discriminate among the individual species by measuring its response to the pure aggregate types (Figure 2a–c), namely, to samples containing monomers, LMW oligomers, HMW oligomers, protofibrils, or fibrils of Aβ_{40} or Aβ_{42}. The concentrations of aggregates used in this experiment (30 μM) were selected after determining the minimal concentrations needed for obtaining maximal fluorescence responses (Figure S1). The different assemblies were prepared according to known protocols (Supporting Information), purified by size exclusion chromatography (SEC), and characterized by Western blotting (Figures 2d and S2) and by transmission electron microscopy (TEM) (Figure S3). Inspecting the fluorescence spectra (Figure 2a) reveals that a strong emission of SRB and sCy5 is observed even in the absence of Aβ aggregates, which could result from direct excitation of SRB, as well as from initial fluorescence of the ThT unit of **1**. These spectra also show that each Aβ sample distinctly affected the response of the different dyes. For example, in the presence of Aβ_{40} fibrils and protofibrils the emission of sCy5 was enhanced at different levels, whereas LMW and HMW oligomers induced a decrease in its emission intensity (Figure 2a, left). At the SRB channel, on the other hand, only a reduction in the emission intensity was observed. With Aβ_{42} different fluorescence responses were detected (Figure 2a, right). The emission of sCy5 was also enhanced in the presence of HMW oligomers and the SRB unit exhibited a differential fluorescence response. Inspecting the emission at different wavelengths reveals that for distinct aggregate types, unique alterations in the level and/or trend of fluorescence were obtained, which has led to the generation of unique optical fingerprints (Figure 2b). Linear discriminating analysis (LDA) was applied to discriminate among these patterns (Figure 2c) and to optimize the conditions

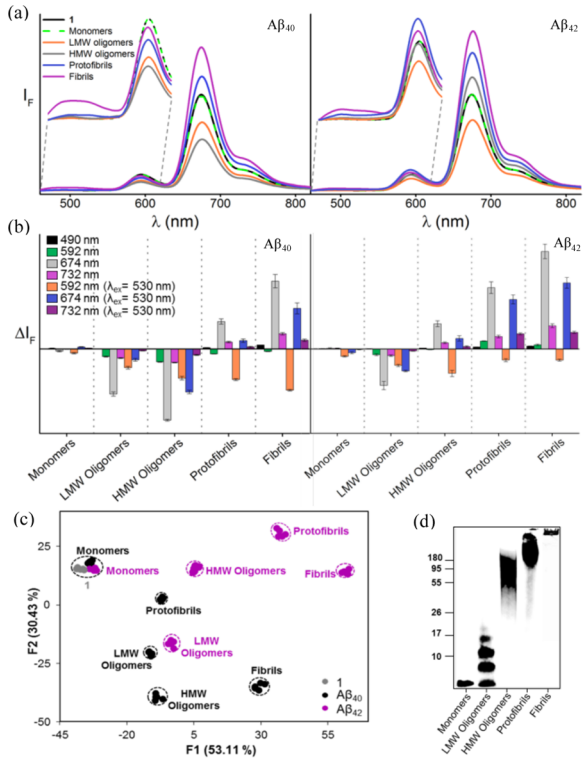

Figure 2. (a) Emission spectra generated by **1** (2 μM, λ_{ex} = 440 nm) in response to the pure aggregate species (30 μM) of Aβ_{40} (left) or Aβ_{42} (right). (b) Patterns obtained by measuring intensity changes at seven representative emission channels (λ_{ex} = 440 and 530 nm). (c) Corresponding LDA plot. (d) Western blot analysis of different Aβ_{40} aggregates.

for classification of samples. For example, LDA has shown that differentiation can be improved by exciting the SRB dye at 530 nm and by acquiring additional data between 560 and 790 nm (Figures 2b,c vs S4). The direct excitation of SRB minimizes the contribution of ThT to the emission patterns, which strengthens the effect of LMW oligomers. The LDA plot was used to identify 20 out of 22 unknown Aβ_{40} and Aβ_{42} aggregate samples (Figure S5), indicating 91% accuracy. To demonstrate the versatility of our approach we have also shown that **1** can discriminate among aggregates of other amyloidogenic proteins, such as lysozyme, prion, insulin, and amylin fibrils (Figure S6).

To confirm the underlying design principles, in particular, the contribution of the specific binders and FRET processes to the discriminatory ability of **1**, several control compounds were prepared and tested against the different Aβ aggregates (Figures 3 and S7). For example, the role that the ThT derivative of **1** plays in sensing Aβ_{40} fibrils (Figure 3a) was assessed by measuring the emission of compound C7, which carries only the ThT dye, in the absence and presence of fibrils (Figure 3b). The large enhancement in the emission signal indicates the suitability of using this derivative for sensing fibrils. Repeating this measurement with compound C21, which possesses both the ThT and the SRB dyes (Figure 3c), has mainly led to an increase in the emission of SRB, confirming the manifestation of an efficient FRET between them. To ensure that this enhancement in SRB fluorescence does not result from the direct response of SRB to fibrils, we repeated the experiment with compounds C20 (Figure 3d) and C28 (Figure 3e), which lack the ThT group. The fact that the emission of these compounds did not change confirmed the critical role that ThT plays in recognizing fibrils,

DOI: 10.1021/jacs.6b10809
J. Am. Chem. Soc. 2017, 139, 2136–2139

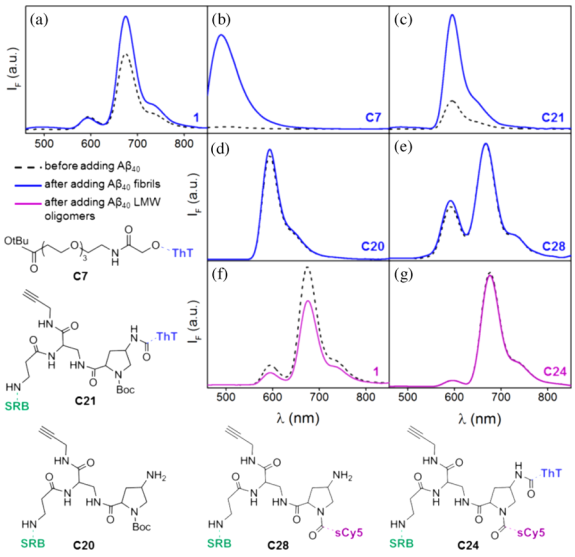

Figure 3. Emission of **1** and control compounds before and after adding fibrils or LMW oligomers. λ_{ex} = 440 nm.

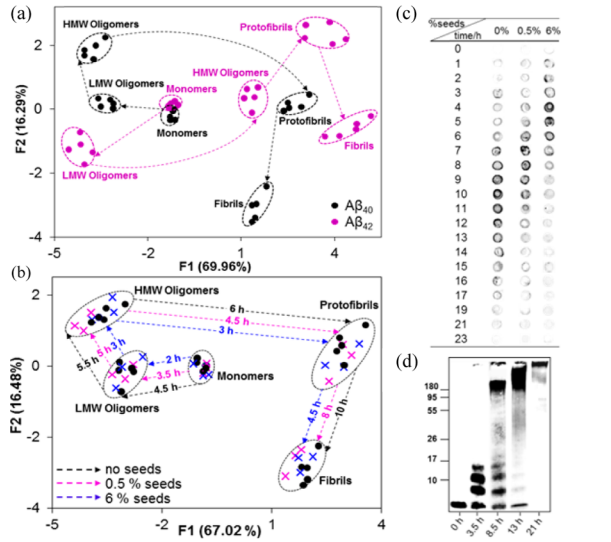

Figure 4. (a) PCA mapping of the patterns generated by **1** when key intermediates of Aβ_{40} or Aβ_{42} are formed. (b) Using PCA to determine the time at which the main aggregate species of Aβ_{40} are formed in the presence of different concentrations of seeds. (c) Dot-blot that follows the formation of HMW oligomers (with oligomer-specific antibody A11) under the same seeding conditions. (d) Western-blot that follows time-dependent changes in the aggregation state of Aβ_{40} in the presence of 0.5% seeds (using anti-Aβ antibody 6E10).

despite the low emission of this dye in the emission spectra of **1** (Figure 3a). Interestingly, the fluorescence of compound C28 was altered upon addition of Aβ_{42} fibrils (Figure S7a), indicating that nonspecific interactions also contribute to the discriminatory ability of **1**. We also showed that this ThT derivative (C7) responds to HMW oligomers and protofibrils, but not to LMW oligomers or monomers (Figure S7b). The contribution of the bis-KLVFF peptide to sensing LMW oligomers was also assessed by measuring the fluorescence response of compound C24, which possesses the three dyes but lacks the bis-KLVFF peptide. Unlike with **1**, in which the emission of SRB and sCy5 was decreased in the presence of LMW Aβ_{40} oligomers (Figure 3f), with C24 the emission of all dyes remained unchanged (Figure 3g).

The strength of differential sensors lies in their ability to discriminate among complex mixtures.[8a] With a unimolecular sensor such as **1**, this property could be particularly useful for following the Aβ aggregation processes, in which the molar ratio between the different Aβ intermediates dynamically changes. To test the ability of the combinatorial sensor to analyze straightforwardly the Aβ aggregation kinetics, we followed the aggregation of Aβ_{40} and Aβ_{42} by measuring the emission of **1** at different time points for 30 h (Figure 4a). In parallel, we followed the formation of the different aggregate species using Western blotting (Figures S8a–I and S9a–I) and dot-blotting (Figure 4c, 0% seeds), which enabled us to associate the fluorescence fingerprints with the formation of key intermediates in the mixture (Figure 4a). To ensure reproducibility, we repeated this experiment five times, starting on different days and from the earliest steps of the protocol, namely, the dissolving of monomers. Examining the clusters in the PCA map (Figure 4a) shows that the system could replicate the emission patterns, which enabled us to differentiate among the main aggregation states of distinct alloforms.

Although Western blot analysis is commonly used to follow changes that occur in the composition of Aβ aggregate mixtures (Figures 4d, S8a-I and S9a-I), this procedure takes more than a day to complete and requires that unstable intermediates be first crossed-linked, which prevents following their formation in real time (Figure S9).

Next, we determined whether, in addition to confirming batch-to-batch reproducibility, the information gained from this analysis could be used to study how changes in the environment affect the structure and dynamics of Aβ_{40} assemblies. Initially, we analyzed the emission generated by **1** in samples that contain increasing concentrations of catalytic seeds (0, 0.5 and 6%, Figure 4b). To confirm that these seeds accelerated the aggregation kinetics, we also used the conventional ThT assay (Figure S8b). Although ThT effectively detected the acceleration in fibril formation, it did not provide any information about other intermediates that were formed. In contrast, inspecting the patterns generated by **1** revealed that although each sample exhibited different kinetics, emission spectra that reflect the formation of the same intermediates were recorded at different time points (Figure 4b). A parallel analysis by Western blotting (Figures S8a and 4d) and dot-blotting (Figure 4c) confirmed that **1** successfully detected the formation of the main aggregate species, although it was not previously tested under these seeding conditions. The relevance of these findings to basic Aβ research was further demonstrated by repeating this experiment with a different concentration of seeds (3%) and by requesting untrained students who were not familiar with these seeding conditions to identify the time at which the intermediates were formed (Figure S10a). Unlike with immunoassays, in which the Aβ aggregates were chemically cross-linked and incubated with primary and secondary antibodies (Figure S10b,c), students that were using **1** were able to track the Aβ intermediates by taking simple fluorescent measurements (Figure S10a).

Another drawback of the prevalent ThT assay is that it is not always suitable for discriminating among aggregates that are generated by distinct pathways, namely, by on-pathways that lead to the formation of fibrils or by off-pathways in which stable nonfibrillar aggregates are formed (Figure 1a). The advantage in using the combinatorial sensor for this purpose has been

DOI: 10.1021/jacs.6b10809
J. Am. Chem. Soc. 2017, 139, 2136–2139

demonstrated by analyzing the emission patterns generated by ThT and **1** in response to different aggregate samples[12] (Figure 5a). On-pathway samples (1-3) correspond to aggregates

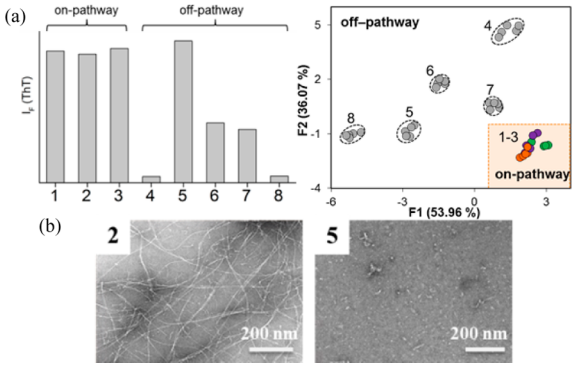

Figure 5. (a) Left: Fluorescence response of ThT to aggregates generated by on (1−3) and off (4−8) pathways. Right: PCA mapping of the patterns generated by **1** in response to the same aggregate samples (samples 1−8). Conditions: 30 μM monomers with (1) no external stimuli, (2) 0.5% seeds, (3) betulinic acid, (4) resveratrol, (5) capric acid, (6) SDS, (7) $Zn(ClO_4)_2$, or (8) $CuCl_2$. (b) TEM images of samples 2 and 5.

formed in the absence (1) and presence of seeds (2) or betulinic acid (3). Off-pathway aggregates (4−8) were prepared by incubating the samples with resveratrol (4), capric acid (5), SDS (6), $Zn(ClO_4)_2$ (7), and $CuCl_2$ (8), all of which have been shown to promote nonfibrillar assemblies.[12] To confirm the structural differences between samples 1−3 and 4−8, we also characterized them by TEM (Figures 5b and S11). As shown in Figure 5a, whereas ThT exhibited "false" "turn-on" responses to some of the off- pathway samples (left, samples 5, 6, and 7), the sensor provided typical fibril signatures only for samples 1−3 (right), demonstrating the viability of this approach.

In conclusion, several advantages of using differential sensing to study Aβ aggregates have been demonstrated using a unimolecular differential sensor. Similar to the widely used ThT assay, **1** is very simple to operate, enabling one to analyze Aβ aggregation states by taking a single fluorescence measurement. Unlike with ThT, however, which mainly responds to fibrils, the combinatorial fluorescent molecular sensor can follow the formation of various different intermediates and can distinguish among alloforms. We have also shown that **1** can differentiate among aggregates generated by different pathways and that it can be used to determine the time at which key intermediates are formed. Considering that our understanding of Aβ fibrillation largely depends on our ability to analyze complex and dynamic mixtures and that the "nose/tongue" approach is particularly useful for analyzing such mixtures, this work indicates the prospect of using combinatorial sensors of this class in Aβ research.

■ ASSOCIATED CONTENT

Supporting Information

The Supporting Information is available free of charge on the ACS Publications website at DOI: 10.1021/jacs.6b10809.

Synthesis of **1**, preparation and characterization of aggregates, and pattern analysis (PDF)

■ AUTHOR INFORMATION

Corresponding Author

*david.margulies@weizmann.ac.il

ORCID

David Margulies: 0000-0002-8151-733X

Notes

The authors declare no competing financial interest.

■ ACKNOWLEDGMENTS

This work was supported by the European Research Council Starting Grant 338265. We thank Dr. Nadav Elad from Department of Chemical Research Support for his help with TEM imaging.

■ REFERENCES

(1) (a) Roychaudhuri, R.; Yang, M.; Hoshi, M. M.; Teplow, D. B. *J. Biol. Chem.* **2009**, *284*, 4749. (b) Rajasekhar, K.; Chakrabarti, M.; Govindaraju, T. *Chem. Commun.* **2015**, *51*, 13434. (c) Haass, C.; Selkoe, D. J. *Nat. Rev. Mol. Cell Biol.* **2007**, *8*, 101. (d) Bitan, G.; Kirkitadze, M. D.; Lomakin, A.; Vollers, S. S.; Benedek, G. B.; Teplow, D. B. *Proc. Natl. Acad. Sci. U. S. A.* **2003**, *100*, 330. (e) Jan, A.; Gokce, O.; Luthi-Carter, R.; Lashuel, H. A. *J. Biol. Chem.* **2008**, *283*, 28176.

(2) (a) Biancalana, M.; Koide, S. *Biochim. Biophys. Acta, Proteins Proteomics* **2010**, *1804*, 1405. (b) Groenning, M. *J. Chem. Biol.* **2010**, *3*, 1.

(3) Teoh, C. L.; Su, D.; Sahu, S.; Yun, S.-W.; Drummond, E.; Prelli, F.; Lim, S.; Cho, S.; Ham, S.; Wisniewski, T.; Chang, Y.-T. *J. Am. Chem. Soc.* **2015**, *137*, 13503.

(4) (a) Li, Q.; Lee, J.-S.; Ha, C.; Park, C. B.; Yang, G.; Gan, W. B.; Chang, Y.-T. *Angew. Chem., Int. Ed.* **2004**, *43*, 6331. (b) Ojida, A.; Sakamoto, T.; Inoue, M.-a.; Fujishima, S.-h.; Lippens, G.; Hamachi, I. *J. Am. Chem. Soc.* **2009**, *131*, 6543. (c) Rajasekhar, K.; Narayanaswamy, N.; Murugan, N. A.; Kuang, G.; Ågren, H.; Govindaraju, T. *Sci. Rep.* **2016**, *6*, 23668. (d) Cao, K.; Farahi, M.; Dakanali, M.; Chang, W. M.; Sigurdson, C. J.; Theodorakis, E. A.; Yang, J. *J. Am. Chem. Soc.* **2012**, *134*, 17338. (e) Cook, N. P.; Torres, V.; Jain, D.; Martí, A. A. *J. Am. Chem. Soc.* **2011**, *133*, 11121.

(5) Lee, J.; Culyba, E. K.; Powers, E. T.; Kelly, J. W. *Nat. Chem. Biol.* **2011**, *7*, 602.

(6) Pedersen, J. T.; Heegaard, N. H. H. *Anal. Chem.* **2013**, *85*, 4215.

(7) Reinke, A. A.; Ung, P. M. U.; Quintero, J. J.; Carlson, H. A.; Gestwicki, J. E. *J. Am. Chem. Soc.* **2010**, *132*, 17655.

(8) (a) Umali, A. P.; Anslyn, E. V. *Curr. Opin. Chem. Biol.* **2010**, *14*, 685. (b) Zamora-Olivares, D.; Kaoud, T. S.; Jose, J.; Ellington, A.; Dalby, K. N.; Anslyn, E. V. *Angew. Chem., Int. Ed.* **2014**, *53*, 14064. (c) De, M.; Rana, S.; Akpinar, H.; Miranda, O. R.; Arvizo, R. R.; Bunz, U. H. F.; Rotello, V. M. *Nat. Chem.* **2009**, *1*, 461. (d) Zhou, H.; Baldini, L.; Hong, J.; Wilson, A. J.; Hamilton, A. D. *J. Am. Chem. Soc.* **2006**, *128*, 2421. (e) Motiei, L.; Pode, Z.; Koganitsky, A.; Margulies, D. *Angew. Chem., Int. Ed.* **2014**, *53*, 9289. (f) Rochat, S.; Gao, J.; Qian, X.; Zaubitzer, F.; Severin, K. *Chem. - Eur. J.* **2010**, *16*, 104.

(9) (a) Rout, B.; Milko, P.; Iron, M. A.; Motiei, L.; Margulies, D. *J. Am. Chem. Soc.* **2013**, *135*, 15330. (b) Rout, B.; Motiei, L.; Margulies, D. *Synlett* **2014**, *25*, 1050. (c) Rout, B.; Unger, L.; Armony, G.; Iron, M. A.; Margulies, D. *Angew. Chem., Int. Ed.* **2012**, *51*, 12477. (d) Sarkar, T.; Selvakumar, K.; Motiei, L.; Margulies, D. *Nat. Commun.* **2016**, *7*, 11374.

(10) Yuen, L. H.; Franzini, R. M.; Wang, S.; Crisalli, P.; Singh, V.; Jiang, W.; Kool, E. T. *Angew. Chem., Int. Ed.* **2014**, *53*, 5361.

(11) (a) Hu, Y.; Su, B.; Kim, C.-S.; Hernandez, M.; Rostagno, A.; Ghiso, J.; Kim, J. R. *ChemBioChem* **2010**, *11*, 2409. (b) Paranjape, G. S.; Gouwens, L. K.; Osborn, D. C.; Nichols, M. R. *ACS Chem. Neurosci.* **2012**, *3*, 302. (c) Wu, C.; Wang, Z.; Lei, H.; Duan, Y.; Bowers, M. T.; Shea, J.-E. *J. Mol. Biol.* **2008**, *384*, 718. (d) Wolfe, L. S.; Calabrese, M. F.; Nath, A.; Blaho, D. V.; Miranker, A. D.; Xiong, Y. *Proc. Natl. Acad. Sci. U. S. A.* **2010**, *107*, 16863.

(12) See Supporting Information for relevant references (Table S1).

DOI: 10.1021/jacs.6b10809
J. Am. Chem. Soc. 2017, 139, 2136−2139